

COB-2023-0195

EXPLORING THE VIBRATION CHARACTERISTICS OF AUXETIC TUBULAR STRUCTURES: AN EXPERIMENTAL ANALYSIS

Adrien Noel

Département des Sciences et Technologies, Haute École Condorcet, Belgium
noel.adrien@hotmail.com

Rafael Augusto Gomes

d2022103026@unifei.edu.br

Lucas Antonio de Oliveira

lucasoliveira2@unifei.edu.br

Sebastião Simões da Cunha Júnior

sebas@unifei.edu.br

Guilherme Ferreira Gomes

Mechanical Engineering Institute, Universidade Federal de Itajubá (UNIFEI), Itajubá, Brazil
guilhermefergom@unifei.edu.br

Abstract. *The exceptional mechanical properties of auxetic structures, known for their negative Poisson's ratio, offer significant improvements compared to conventional structures. The present study conducted a comprehensive analysis and comparison of the vibration responses in three auxetic tubular structures, all sharing identical parameters but featuring distinct unit cell models: Reentrant, Double-V, and Anti-Trichiral. Vibration tests were systematically executed on standardized samples with uniform dimensions in terms of diameter and height. These tests employed two different materials: PLA and PLA-Carbon filament. The ensuing free vibration tests furnished essential modal data regarding natural frequency and structural damping. The experimental outcomes revealed that auxetic tubular structures fabricated from PLA reinforced with carbon fiber exhibited superior stiffness and damping properties when contrasted with their PLA counterparts. As a result, the reentrant unit cell configuration displayed a 5% and 8% improvement in damping capacity compared to the Double-V and Anti-Trichiral structures, respectively, when using PLA. When utilizing PLA-Carbon, the reentrant unit cell arrangement demonstrated 4% and 23% enhancement in damping capabilities relative to the Double-V and Anti-Trichiral structures, respectively. This study delivers valuable insights into the behavior of diverse auxetic cell types composed of two different materials when subjected to vibrational forces within tubular structures.*

Keywords: *Auxetic, Tubular Structure, Additive Manufacture, Vibration Analysis.*

1. INTRODUCTION

Over the years, there has been a need for development in structural engineering of new materials and structures that meet the high specifications of engineering projects in the aeronautical, automotive, medical, sports, and even leisure sectors. Structures that exhibit exceptional mechanical properties and performance beyond those of conventional structures have received increasing attention (Alderson and Alderson (2007))

In contrast, due to their superior mechanical properties, structures and materials with negative Poisson's ratio (NPR) behavior have drawn more interest from researchers worldwide. According to Evans and Alderson (2000), it is normal to expect that a common material will lengthen in the direction of the strain and thin out in cross-section when it is stretched. Most common materials, such as rubber, steel, and carbon, have a positive Poisson's ratio (PPR), indicating that they expand under compression and contract under traction. This behavior is determined by Poisson's ratio (ν), one of the material's fundamental mechanical properties. Therefore, materials and structures made of negative Poisson's ratio (NPR) exhibit an unusual behavior in which they contract transversely under compression and expand transversely under traction. This behavior of the material is also determined by the Poisson's ratio. The first foam with an NPR behavior was described in 1987 by one of the pioneers, Lakes (1987), and later researchers, Evans *et al.* (1991) referred to this structure as auxetic (from the Greek *auxetos*), which means inclined to increase.

Auxetic tubular structures, in comparison to traditional tubular structures, exhibit a range of desirable mechanical characteristics such as energy absorption ability, bending performance, and twist deformation. Researchers conducted worldwide, including studies by Ren *et al.* (2022); Scarpa *et al.* (2003) and Farokhi Nejad *et al.* (2020), has explored their energy absorption capabilities. Additionally, Scarpa *et al.* (2008) and Abbaslou *et al.* (2023) have delved into their bending performance. Evans and Alderson (2000) examined shear modulus and identification resistance, while Farrell

et al. (2020) analyzed twist deformation. Moreover, Lakes and Elms (1993) conducted research on enhanced fracture toughness in auxetic materials. These studies collectively underscore the advantages and potential applications of auxetic tubular structures in the field of engineering and materials science.

One of the characteristics of auxetic structures is that they have, in most cases, complex geometries to achieve auxetic behavior. According to Gomes *et al.* (2023), it has become possible to design and produce auxetic structures utilizing conventional materials made of positive Poisson's ratio materials because of the development of manufacturing processes like 3D printing, which can produce complex geometry. The configuration of the unit cell designs utilized in the structure, which is responsible for providing a negative Poisson's ratio behavior, can make this possible. As explained by Francisco *et al.* (2022), these structures have been offered and developed by writers all over the world since the first structure, Reentrant; following this, numerous other structures, including Chiral, Anti-Chiral, Double-V, Perforated models, S-shape, and Missing-rib structures, were also proposed. These models each have benefits and drawbacks, and the geometry and material that are used will depend on the structure's intended use and the manufacturing equipment that is available.

In the current study, we compare three auxetic tubular structures made up of different types of unit cells, being Double-V, Reentrant, and Anti-Trichiral, in order to analyze the vibration behavior of auxetic tubular structures while adhering to the step-by-step technique suggested by Gomes *et al.* (2023). The samples used in our study have identical parameters of diameter and height, and we analyze their efficiency based on weight. They were also manufactured using a 3D printer with PLA and PLA+Carbon filament materials. The modal testing was performed in order to obtain both the time and frequency response domains where the modal parameters: natural frequency and structural damping were obtained. The obtained findings presented the vibration behavior of auxetic tubular structures and also made it possible to compare the structures with different unit cells composed of different materials. The results provide valuable insights into the natural frequency analyzed by the FRF, and using the decrement logarithmic methodology, it was possible to calculate the damping of the auxetic tubular structures.

2. METHODOLOGY

2.1 MODEL

Three different types of auxetic tubular tubes were developed and assessed, using weight as a criterion to examine the vibration behavior of the structures. The unit cells used in the tubular devices were modeled on popular auxetic unit cells that have been proposed around the world, specifically the Double-V (DV) unit cell from a work cited in Gao *et al.* (2018), the Reentrant (RE) unit cells investigated in earlier research by Francisco *et al.* (2023), as well as Anti-Trichiral (TCH), which was based on the unit cells suggested by Hu *et al.* (2019). The auxetic tubular structures were developed using a commercial CAD software, and the unit cells in the standardized tubular structure were indicated to have the following dimensions: 300 mm in height, 30 mm in external diameter, and 1.6 mm in thickness, which resulted in three different kinds of auxetic tubular structures. Figure 1 presents the auxetic tubular structural models.

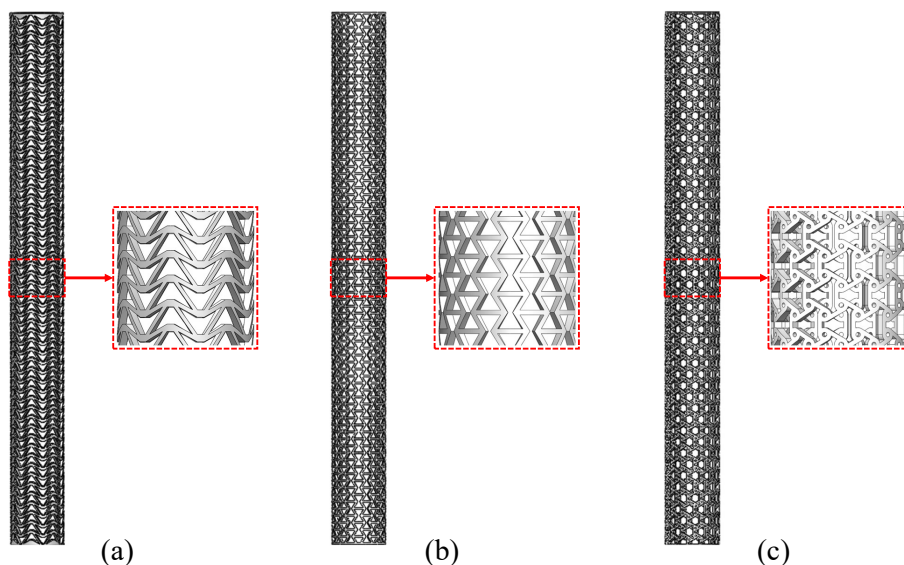


Figure 1. Auxetic tubular structures models: (a) Double-V (DV); (b) Reentrant (RE); (c) Anti-Trichiral (TCH)

2.2 SAMPLES MANUFACTURING

The samples of auxetic tubular devices were created via additive manufacturing on the Trevo Tornado printer using polylactic acid (PLA) filament and PLA with carbon, both of which have a 1.75 mm diameter. The printing temperature and the build plate temperature are equal to 200 °C and 60 °C, respectively. Layer height, print speed, and infill density are all set to 30 mm/s, 0.2 mm, and 100%, respectively. The structures were designed in CAD software and posteriorly imported into the Ultimaker CURA[®] software, where all of the printing configurations were made. In Fig. 2, it is possible to see a part of the manufacturing process of the auxetic tubular structures.

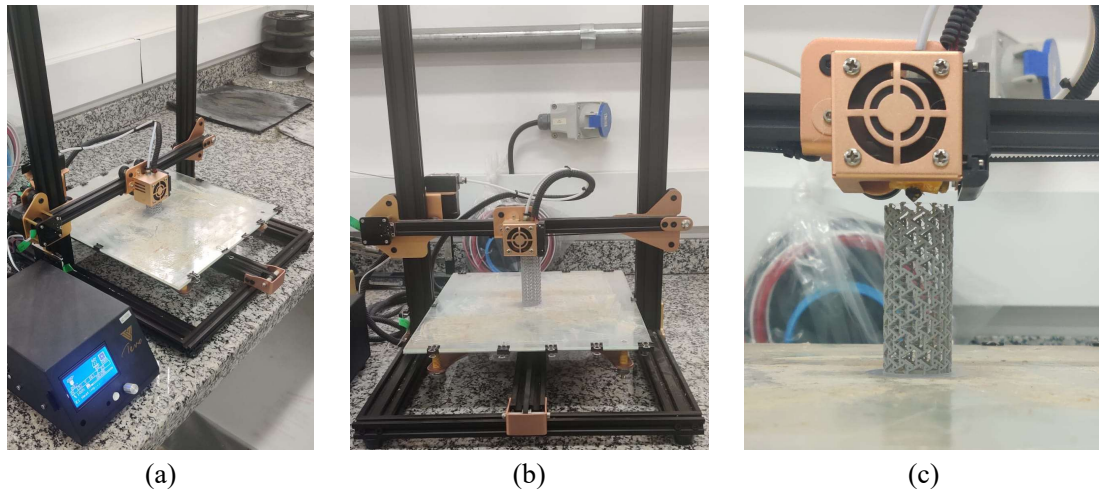


Figure 2. (a) Trevo Tornado printer; (b) printing process; (c) printing detail of an Anti-Trichiral auxetic tubular structure.

2.3 EXPERIMENTAL TEST

The vibration test presented in Fig. 3 was utilized to conduct the test on all specimens (Reentrant, Double-V, and Anti-Trichiral) to study the vibration behavior including the structural damping of the auxetic tubular structures. The base extremities of the samples were fastened with a 3-point support clamp. To perform the structural excitation, a miniature impact hammer, Bruel & Kjaer 8204, with 22.7 MV/N, was utilized. Posteriorly, to measure the vibration of the structure, a vibration testing machine, an Ometron VQ-500-D Laser Vibrometer, was also utilized, together a portable dynamic signal analyzer Bruel & kjaer Photon + with four inputs. And finally, all the collected data during the experiment could be monitored using the Data Recorder software.

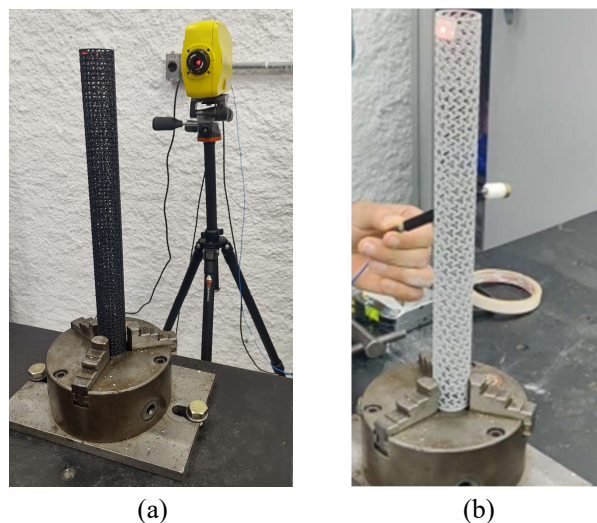


Figure 3. Vibration experimental test: (a) Setup of the experimental test; (b) Experimental test procedure.

3. RESULTS AND DISCUSSION

3.1 Natural Frequency

After performing the experimental vibration tests, it was possible to obtain the Frequency Response Function (FRF), where the analysis of the FRF data is presented in Fig. 4 for the PLA structure and in Fig. 5 for the PLA+Carbon structure. It allows us to observe the behavior of the three types of auxetic unit cells, Double-V, Reentrant, and Anti-Trichiral, applied in tubular structures, allowing us to observe the range of natural frequencies acquired by the vibration test.

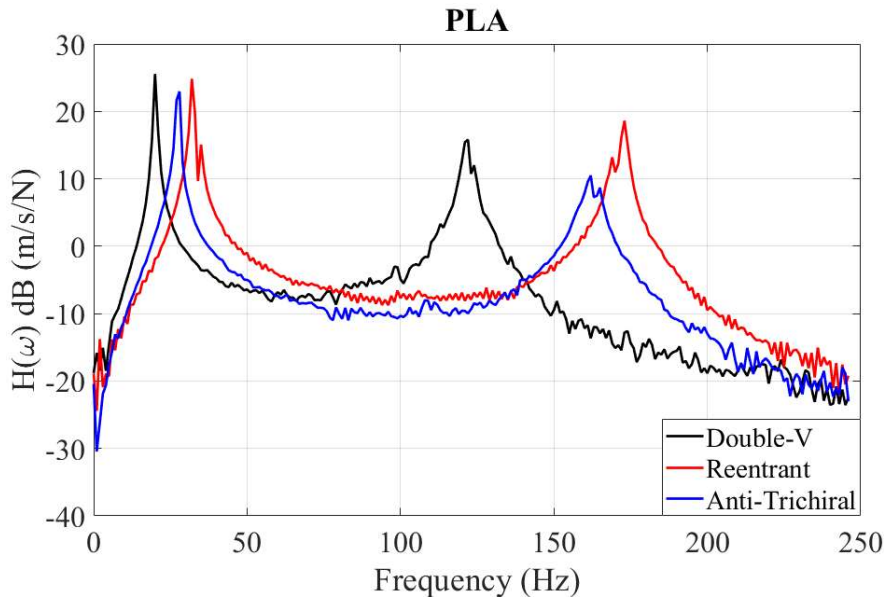


Figure 4. Vibration FRF results for the auxetic tubular structures for samples composed of PLA filament material

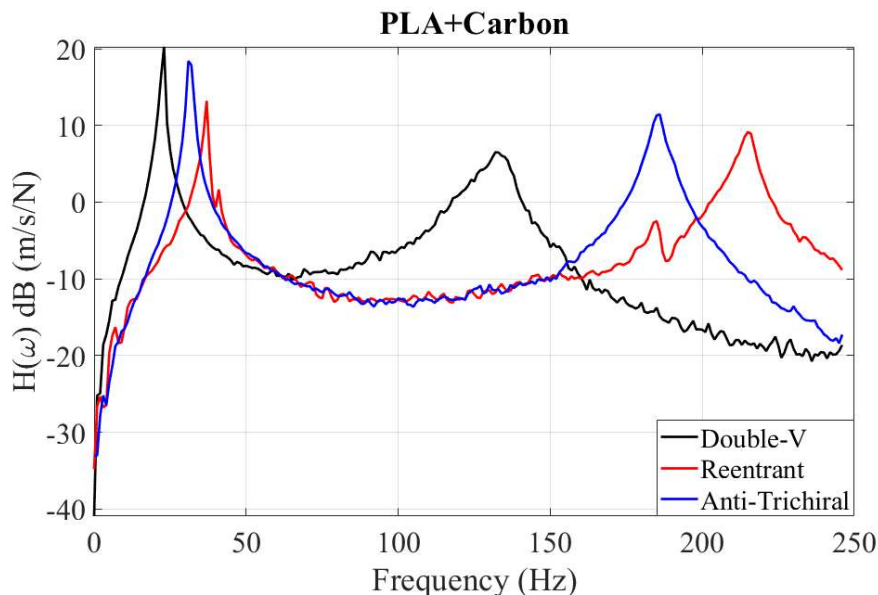


Figure 5. Vibration FRF results for the auxetic tubular structures for samples composed of PLA+Carbon filament material

Equally important, Fig. 6 presents the comparison of the material influence of the samples devices using PLA filament vs. PLA+Carbon filament due to the FRF signal analysis in the Double-V, Reentrant, and Anti-Trichiral structures, where the samples had the same parameters and dimensions and were tested in the same temperature and pressure conditions. It is possible to note that the change of material implies a change in the specific mass and also a change in the stiffness of the material, consequently the natural frequency of vibration of each proposed structure. The results extracted from the vibration signal of the auxetic tubular structures tested can be observed in Tab. 1, which compares the unit cell used, the material, and the natural frequency obtained.

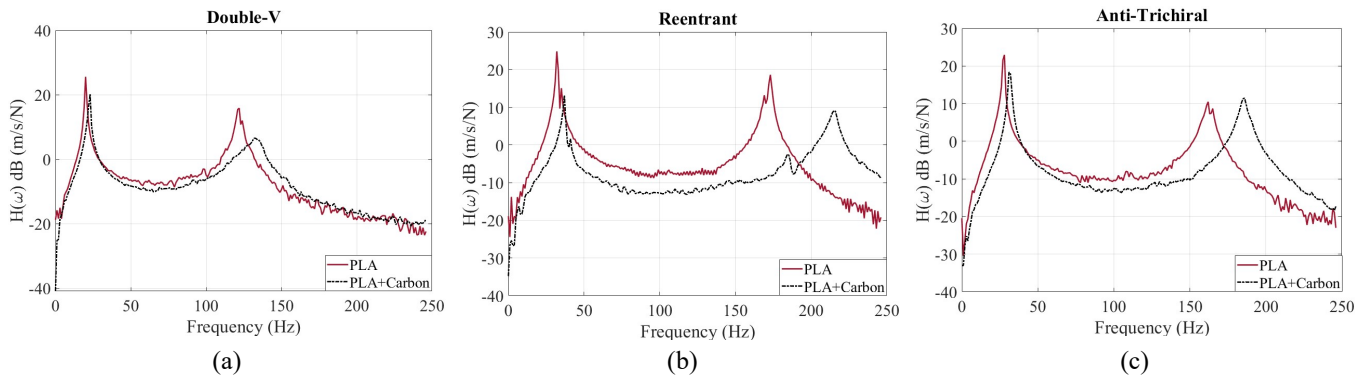


Figure 6. FRF of the vibration experimental test results for the auxetic tubular structures, comparing the samples for different materials: (a) Double-V, (c) Reentrant, and (c) Anti-Trichiral.

Table 1. Experimental results, obtained by the FRF of auxetic tubular structures

Model	Material	Mass (g)	ω_n1 (Hz)	ω_n2 (Hz)
Double-V	PLA	20.63	20	122
	PLA-Carbon	21.35	23	132
Reentrant	PLA	20.51	32	173
	PLA-Carbon	21.58	37	215
Anti-Trichiral	PLA	20.81	28	162
	PLA-Carbon	21.14	31	185

From analyzing the results presented in Table 1, it is possible to note that samples composed of PLA-Carbon presented the highest stiffness compared to PLA. Therefore, when comparing the unit cells, better stiffness is observed in the samples composed of Reentrant unit cells compared to the Double-V and Anti-Trichiral. It is possible to determine from the observation of the highest natural frequency among the structures.

3.2 Structural Damping

To evaluate the damping ability of the structures were used the logarithmic decrement method. Where the term "decrement logarithmic" refers to the rate of logarithmic reduction in movement after an impulse when energy is distributed to other components of the system or absorbed by the element itself. According to COSSOLINO and PEREIRA (2010), the structural damping represented by ζ , using the logarithmic decrement, can be calculated using the Eq. 1:

$$\zeta = \frac{1}{\sqrt{1 + (2\pi/\delta)^2}} \quad (1)$$

where the value of the logarithmic decrement delta (δ) is obtained by the Eq. 2, where (A_1) is expressed by the amplitude of the first peak, (A_n) is expressed by the amplitude of the last peak, and (n) is the number of peaks.

$$\delta = \frac{1}{n} \cdot \ln \left(\frac{A_1}{A_n} \right) \quad (2)$$

Figure 7, presents a time response plot of the data collected by the vibration experimental test, which compares the behavior of the samples with different auxetic unit cells manufactured using PLA in Fig. 7 (a) and PLA+Carbon filament in Fig. 7 (b).

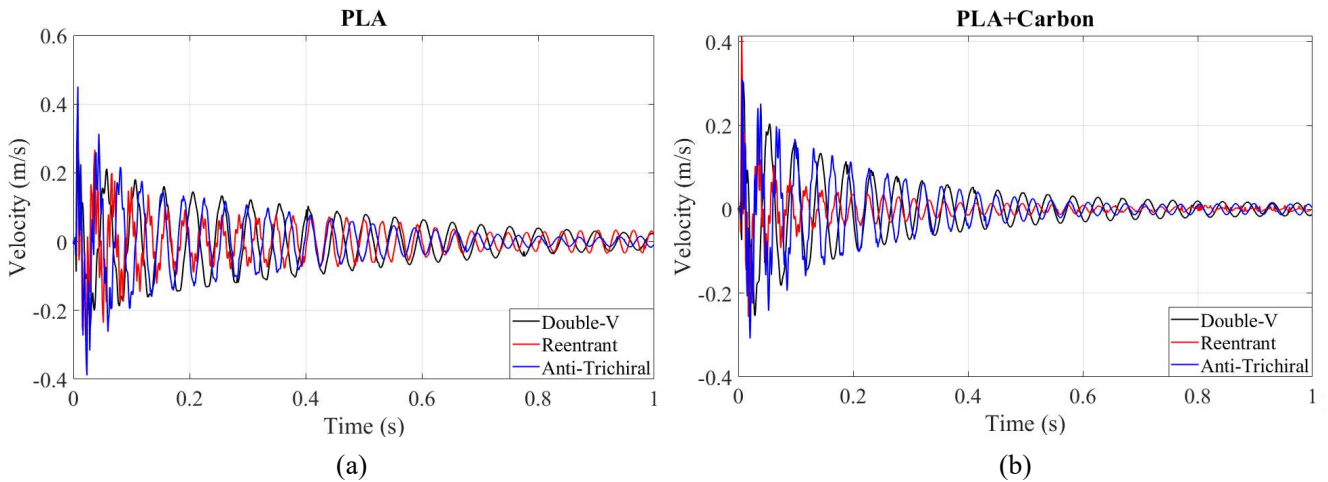


Figure 7. Vibration time response results for the auxetic tubular samples: (a) manufactured with PLA; (b) manufactured with PLA+Carbon.

Fig. 8 shows the material and geometry influence in the structural damping. The samples were tested under the same temperature and pressure conditions and had the same parameters and dimensions. It is possible to note that when analyzing the time response of the samples in all cases, the structures composed of Reentrant unit cells with PLA-Carbon material presented the highest damping ability when compared to the other structures. Which is an important feature when performing a modal analysis.

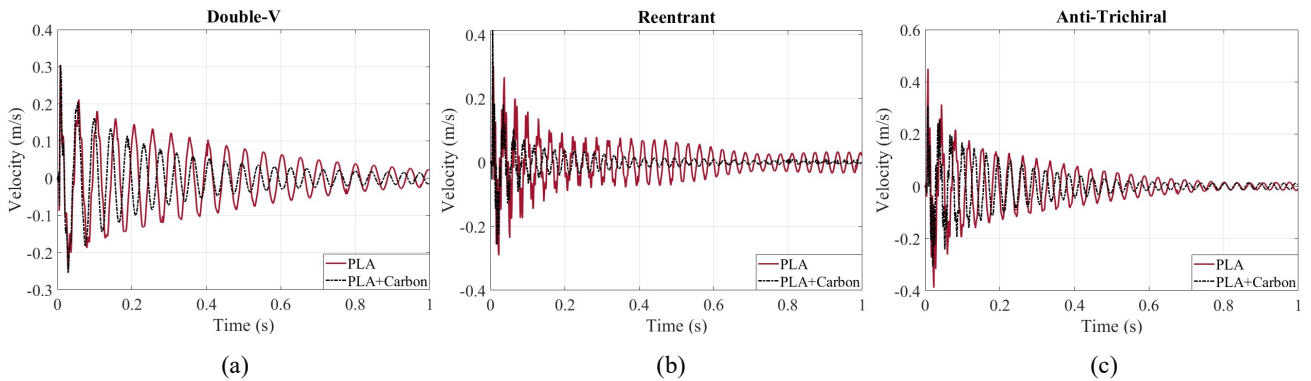


Figure 8. Time response of the vibration experimental test results for the auxetic tubular structures, comparing the samples for different materials: (a) Double-V, (b) Reentrant, and (c) Anti-Trichiral.

Finally, Tab. 2 presents the comparative value of structural damping obtained by the logarithmic decrement method from Figs. 7, and 8, for the three types of auxetic structures. As a result, the reentrant unit cell configuration displayed a 5% and 8% improvement in damping capacity compared to the Double-V and Anti-Trichiral structures, respectively, when using PLA. When utilizing PLA-Carbon, the reentrant unit cell arrangement demonstrated 4% and 23% enhancement in damping capabilities relative to the Double-V and Anti-Trichiral structures, respectively.

Table 2. Results obtained by calculating the structural damping of auxetic tubular structures using the logarithmic decrement method

Model	Material	Mass (g)	Structural Damping (%)
Double-V	PLA	20.63	2.02
	PLA-Carbon	21.35	2.77
Reentrant	PLA	20.51	2.13
	PLA-Carbon	21.58	3.00
Anti-Trichiral	PLA	20.81	2.04
	PLA-Carbon	21.14	2.31

4. CONCLUSION

The auxetic tubular structures have attracted significant attention from all over the world due to their exceptional mechanical properties. In the current study, using weight as a parameter, it was possible to investigate the performance of three different auxetic tubular structures composed by Double-V, Reentrant, and Anti-Trichiral vibration tests.

The results showed the comparison of the auxetic tubular structure behavior during the vibration experimental test, which allowed the analysis of the natural frequency and structural damping of the three applied geometries. The auxetic tubular structure composed of Reentrant unit cells presented the best capacity for damping when compared to the other structures, Double-V and Anti-Trichiral. In addition, the PLA+Carbon filament did not significantly enhance the structural properties of the auxetic tubular structures compared to pure PLA filament; furthermore, future studies should be developed to ratify the comparison of the mechanical properties of both materials.

Finally, it is possible to conclude that the auxetic tubular structures exhibit many excellent mechanical properties, making it highly interesting to research the benefits and opportunities to be developed. These structures are actually anticipated to become more common in the near future and may play significant roles in a variety of engineering fields and industries, including mechanical, naval architecture, aerospace, automotive, and medical.

5. ACKNOWLEDGEMENTS

The authors would like to acknowledge the financial support from the Brazilian agency CNPq (Conselho Nacional de Desenvolvimento Científico e Tecnológico - 431219/2018-4), CAPES (Coordenação de Aperfeiçoamento de Pessoal de Nível Superior) and FAPEMIG (Fundação de Amparo à Pesquisa do Estado de Minas Gerais - APQ-00385-18). The authors would also like to acknowledge Tutorial Education Program (PET – Programa de Educação Tutorial).

6. REFERENCES

- Abbaslou, M., Hashemi, R. and Etemadi, E., 2023. “Novel hybrid 3d-printed auxetic vascular stent based on re-entrant and meta-trichiral unit cells: Finite element simulation with experimental verifications”. *Materials Today Communications*, Vol. 35, p. 105742.
- Alderson, A. and Alderson, K., 2007. “Auxetic materials”. *Proceedings of the Institution of Mechanical Engineers, Part G: Journal of Aerospace Engineering*, Vol. 221, No. 4, pp. 565–575.
- COSSOLINO, L.C. and PEREIRA, A.H.A., 2010. “Amortecimento: classificação e métodos de determinação”. *Universidade de São Carlos*.
- Evans, K.E. and Alderson, A., 2000. “Auxetic materials: functional materials and structures from lateral thinking!” *Advanced materials*, Vol. 12, No. 9, pp. 617–628.
- Evans, K.E., Nkansah, M., Hutchinson, I. and Rogers, S., 1991. “Molecular network design”. *Nature*, Vol. 353, No. 6340, pp. 124–124.
- Farokhi Nejad, A., Alipour, R., Shokri Rad, M., Yazid Yahya, M., Rahimian Koloor, S.S. and Petr, M., 2020. “Using finite element approach for crashworthiness assessment of a polymeric auxetic structure subjected to the axial loading”. *Polymers*, Vol. 12, No. 6, p. 1312.
- Farrell, D.T., McGinn, C. and Bennett, G.J., 2020. “Extension twist deformation response of an auxetic cylindrical structure inspired by deformed cell ligaments”. *Composite Structures*, Vol. 238, p. 111901.
- Francisco, M.B., Pereira, J.L.J., da Cunha Jr, S.S. and Gomes, G.F., 2023. “Design optimization of a sandwich composite tube with auxetic core using multiobjective lichtenberg algorithm based on metamodelling”. *Engineering Structures*, Vol. 281, p. 115775.
- Francisco, M.B., Pereira, J.L.J., Oliver, G.A., Roque da Silva, L.R., Cunha Jr, S.S. and Gomes, G.F., 2022. “A review on the energy absorption response and structural applications of auxetic structures”. *Mechanics of Advanced Materials and Structures*, Vol. 29, No. 27, pp. 5823–5842.
- Gao, Q., Zhao, X., Wang, C., Wang, L. and Ma, Z., 2018. “Multi-objective crashworthiness optimization for an auxetic cylindrical structure under axial impact loading”. *Materials & design*, Vol. 143, pp. 120–130.
- Gomes, R.A., de Oliveira, L.A., Francisco, M.B. and Gomes, G.F., 2023. “Tubular auxetic structures: A review”. *Thin-Walled Structures*, Vol. 188, p. 110850.
- Hu, L., Ye, W. and Wu, Z., 2019. “Mechanical property of anti-trichiral honeycombs under large deformation along the x-direction”. *Thin-Walled Structures*, Vol. 145, p. 106415.
- Lakes, R., 1987. “Foam structures with a negative poisson’s ratio”. *Science*, Vol. 235, No. 4792, pp. 1038–1040.
- Lakes, R. and Elms, K., 1993. “Indentability of conventional and negative poisson’s ratio foams”. *Journal of Composite Materials*, Vol. 27, No. 12, pp. 1193–1202.
- Ren, X., Zhang, Y., Han, C.Z., Han, D., Zhang, X.Y., Zhang, X.G. and Xie, Y.M., 2022. “Mechanical properties of foam-filled auxetic circular tubes: Experimental and numerical study”. *Thin-Walled Structures*, Vol. 170, p. 108584.
- Scarpa, F., Ciffo, L. and Yates, J., 2003. “Dynamic properties of high structural integrity auxetic open cell foam”. *Smart*

materials and structures, Vol. 13, No. 1, p. 49.

Scarpa, F., Smith, C., Ruzzene, M. and Wade, M., 2008. "Mechanical properties of auxetic tubular truss-like structures".
physica status solidi (b), Vol. 245, No. 3, pp. 584–590.

7. RESPONSIBILITY NOTICE

The author(s) is (are) the only responsible for the printed material included in this paper